OPTOSKY
www.optosky.com

Datasheet

Drone Hyperspectral Imaging System

ATHL9010

Features:

- Range: 400~1000nm
- Spectral Resolution: < 1.5 nm
- FOV: 23.5°@f=35mm (Lens changeable)
- IFOV：0.9 mrad@f=35mm (Lens changeable)
- Flight height: 50~1000 m, recommend height 100m
- Solid state LiDAR with high reliability
- LiDAR measure range: 1~200m
- LiDAR measure height error: 20 mm
- PC Intel Core i7 with max. 2T memory reach up to 100 hours images data
- 1.5m multi-wing drone with heavy-load or extendable
- Long flight time about 45 minutes, large cruise area

Application:

- **Monitor Agriculture:** plant diseases and insect pest, disaster, categories ID etc.
- **Forestry:** Tree categories identification, Phytomass, nutrient elements, forest health etc.
- **Water Environment:** Water quality parameters, water waste spatial distribution and migration analysis
- **Soil Pollution:** heavy metal waste
- **Minerals:** Mineral mapping, ingredients explore, metallogenic prognosis etc.
- **City geological:** substances classification and identification

Description:

ATHL9010 series is the 3rd generation hyperspectral imager integrated LiDAR system. This new series feature compact and light.

It consists of eight main parts of six-rotor UAV, high-stable cloud platform, hyperspectral imager, LiDAR, big memory storage, GPS navigation system, ground receiver station, and ground control system.

It depends on linear LiDAR to get surface elevation, images ortho-rectification, and 3D object attitude, whose LiDAR data and spectral data are being combined to analysis open up new research way.

ATHL9010 integrated high-precision hyperspectral imager and high-resolution LiDAR, which generates field true color point cloud, one fly can get as fast as >2 km2 point cloud data.

From real-time measure spetral data collection to spectral images analysis, and final physicochemical properties calculation. They've widely applied to plants classification and growth assessment.

1. Selection

Model	Description
ATHL9010	standard resolution
ATHL9010P	High SNR
ATHL9010W	Wider FOV

2. Technical Specification

OPTOSKY
www.optosky.com

Datasheet

	ATHL9010	ATHL9010P	ATHL9010W
UAV System			
Drone	Luxury Six Rotor Drone customized with load hour > 45 minutes		
Cloud Platform	High stable Cloud platform driven by 3-Phase BLDC Motor		
Rotor No.	Six Rotors		
Lift	Take off and land vertically		
Wheelbase	1500 mm		
Max base	6 Kg		
Max altitude	5000 m		
Drone size	1650 X 1410 X 500 mm		
GPS accuracy	1.5 m	0.5 m	<0.3m，RTK
Remote change imaging specs (Y/N)	No	Yes	Yes
Flight duration	>45 minutes	>45 minutes	>45 minutes
Ground control distance	5 Km	10 Km	10 Km
Hyperspectral Imager			
Interface	USB3.0	USB3.0	USB3.0
Imaging mode	Push broom		
Resolution Before Binning	1920（spatial-axis） × 1200（spectral-axis）	1920（spatial-axis）× 1080（spectral-axis）	2048（spatial-axis）× 2048（spectral-axis）
Resolution After Binning	480（spatial-axis）×300（spectral-axis）	480（spatial-axis）×270（spectral-axis）	512（spatial-axis）×512（spectral-axis）
Max frame rate	270 Hz	130 Hz	180 Hz
Load PC	Intel I7 CPU 16G		
PC Hard drive	512 GB SSD，Max 2T		
Image resolution	1920 × 1200	1920×1080	2048×2048
Power supply	12V，3W	12V，5W	12V，5W
LiDAR			
Principle	The LIDAR system uses the time of flight(TOF) to measure the distance		
Laser	1550nm Eye-safe		
Speed	500,00 points per second, max 1,000,000 points per second depends on the distance		
Scan Line	1750 lines		
FOV	Horizontal 15°□		
Angular resolution	Horizontal 0.009°□		
Scan rate	500 Hz		
Elevation	1~300 m，Max 600 m		
Laser return mode	Multiple returns		
Altitude deviation	<20 mm		
Weight	1.5 Kg		
Reliability			
Working Temp	-10 ~ 45℃		
Storage Temp	-20 ~ 65℃	-20 ~ 65℃	-20 ~ 65℃
Working Humidity	≤85% RH	≤85% RH	≤85% RH
Optical Parameters（customization option）			
Spectral range	400~1000 nm (customization option)	400~1000 nm (customization option)	400~1000 nm (customization option)
Resolution	< 1.5 nm	< 1.5 nm	< 1.5 nm
Smile	<1/3 pixel	<1/3 pixel	<1/3 pixel

Keystone	<1/3 pixel	<1/3 pixel	<1/3 pixel
Lens FL	35mm	35mm	35mm
FOV	15.2°	14.6°	21.6°
Slit size	30μm	30μm	30μm
NA	0.19(F/2.6)	0.2(F/2.4)	0.2(F/2.4)
Optical bench	PG imaging spectrometer	PG imaging spectrometer	PG imaging spectrometer
Sensor			PG imaging spectrometer
Type	CMOS	CCD	CMOS
Range	350~1100 nm	350~1100 nm	350~1100 nm
Effective pixel	1920 × 1200	1920×1080	2048×2048
Dynamic range	60 dB	66 dB	72 dB
Bit depth	12 bit	12bit	12bit
Mode	Software Binning or hardware binning（software setup）	Software Binning or hardware binning（software setup）	Software Binning or hardware binning（software setup）
PC	I7，16G ，512GB，Max 2TB		
Visible camera			
Resolution	2-mega pixels		
Frame rate	20 FPS		
Software			
Basic Functions	Flexible to set exposure time, gain, speed, dynamic real-time images and curves	Flexible to set exposure time, gain, speed, dynamic real-time images and curves	Flexible to set exposure time, gain, speed, dynamic real-time images and curves
Focus adjust	Dynamic real-time image obtained through precision focus adjustment can avoid human visual focusing error	Dynamic real-time image obtained through precision focus adjustment can avoid human visual focusing error	Dynamic real-time image obtained through precision focus adjustment can avoid human visual focusing error
Software Functions	Data acquire software can real-time shows images and curves Transmission and reflectance measure mode set exposure time, speed in flexible Standard in-built Library and self-built library Others like images cut and identify spectrum	Data acquire software can real-time shows images and curves Transmission and reflectance measure mode set exposure time, speed in flexible Standard in-built Library and self-built library Others like images cut and identify spectrum	Data acquire software can real-time shows images and curves Transmission and reflectance measure mode set exposure time, speed in flexible Standard in-built Library and self-built library Others like images cut and identify spectrum

3. Attachment Lists

N/A	Item	Amount	Comment
1	Hyperspectral Imager（400-1000nm）	1	Standard
2	LiDAR	1	Standard
3	Six-rotor UAVs	1	Standard
4	Could platform and Landing Gear Systems	1	Standard
5	Data-based acquisition and storage system	1	Standard
6	Battery pack and Objective lenses	1	Standard
7	Hyperspectral Imaging System workstation	1	Standard

	(including operating controller and control software)		
8	95% reflectivity, Standard white plate Φ50cm	1	Standard
9	A cloud platform of High precision indoor scanning	1	Optional
10	High stable halogen lamp	4	Optional
11	Standard Calibration Board	1	Optional
12	Imported Calibration Cloth for field (1.2m×1.2m)	1	Optional
13	360-degree rotating platform	1	Optional
14	Tripod	1	Optional
15	High capacity lithium ion batteries	2	Optional
16	Darkroom	1	Optional
17	ortable transport box	1	Optional
18	The device of Pushbroom	1	Optional

4. Airborne Hyperspectral System

OPTOSKY
www.optosky.com

Datasheet

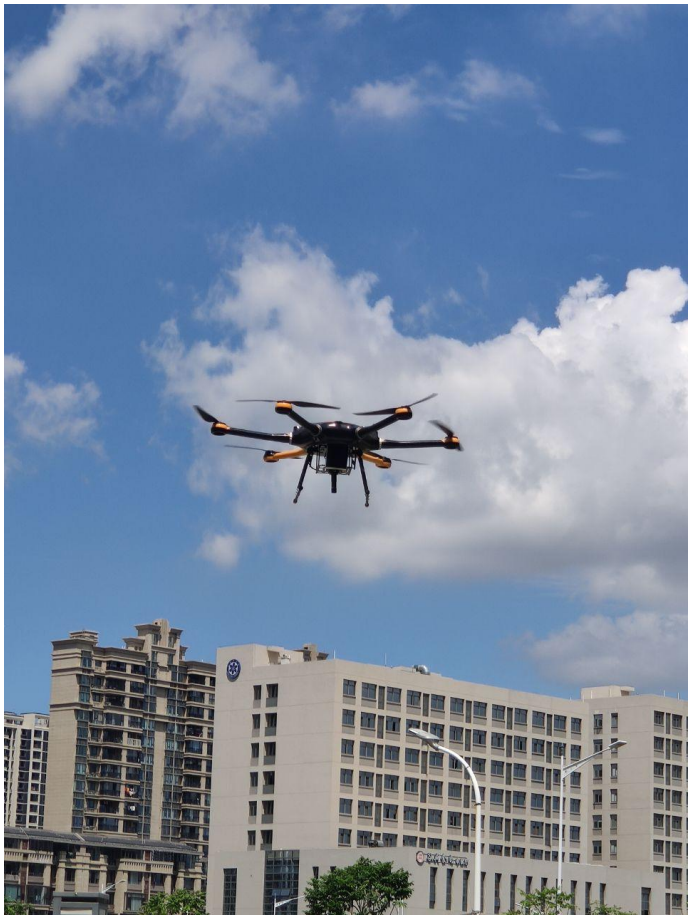

5. Flight Data Record

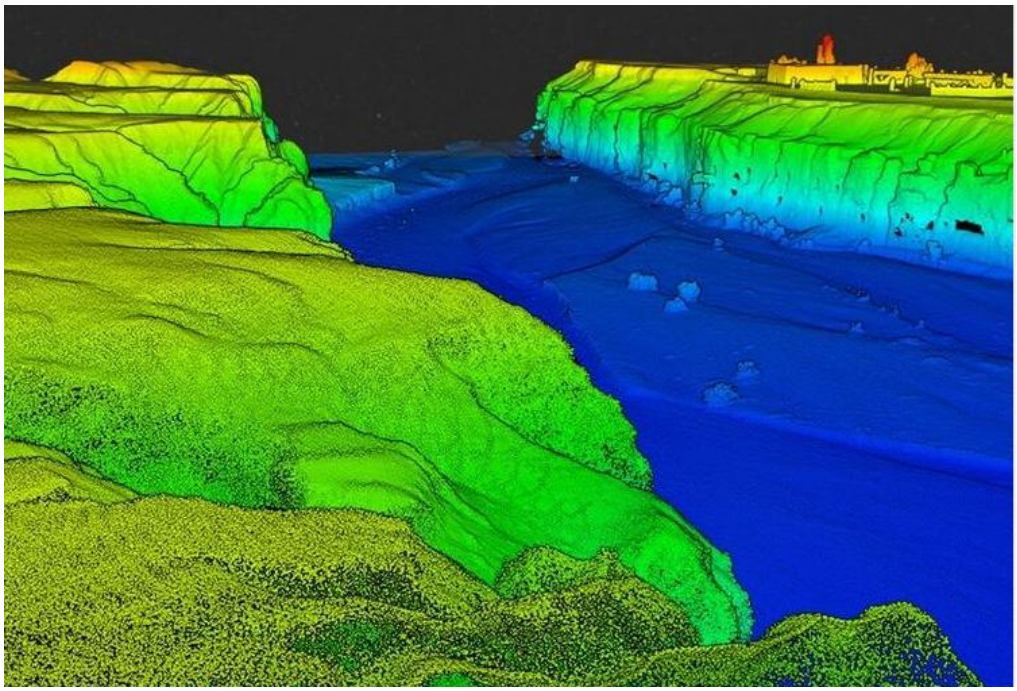

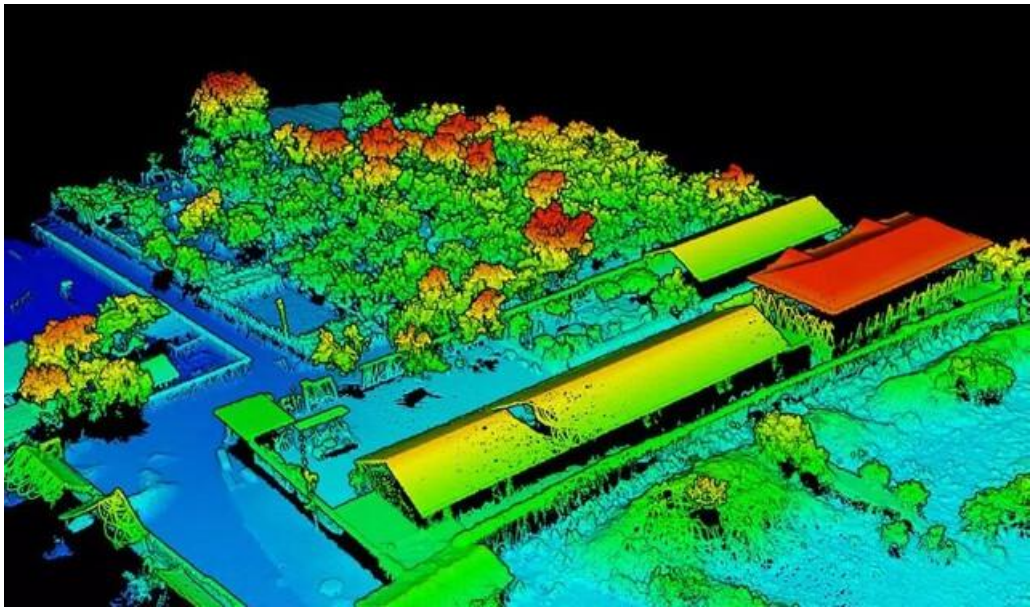

OPTOSKY
www.optosky.com

Datasheet

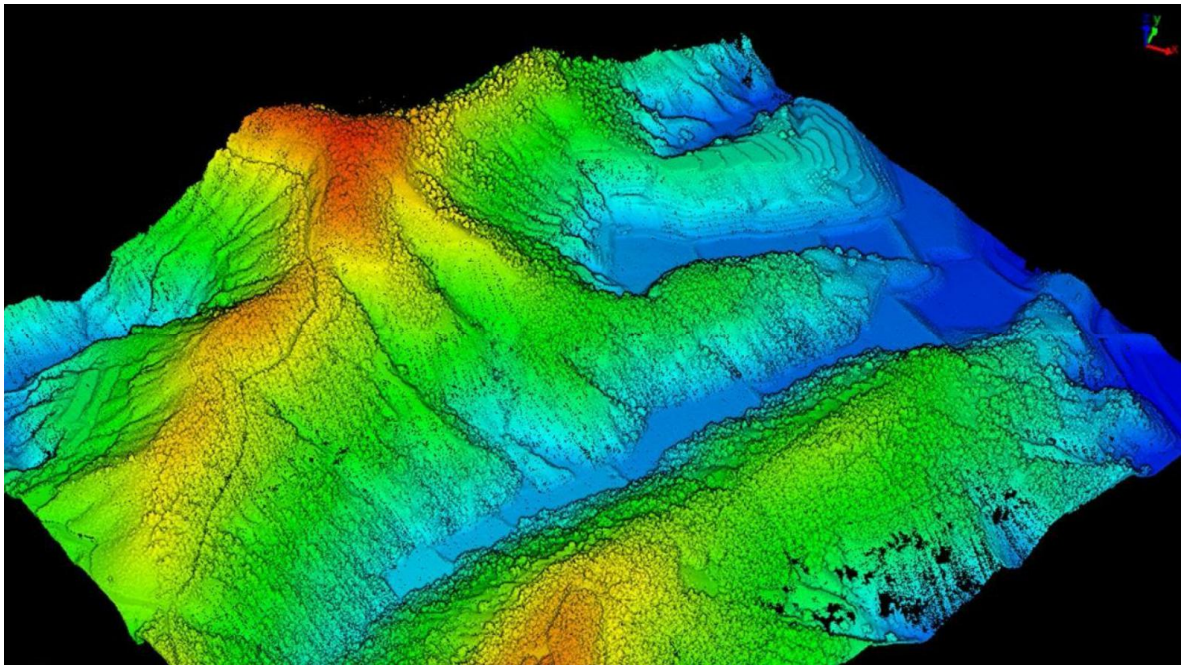

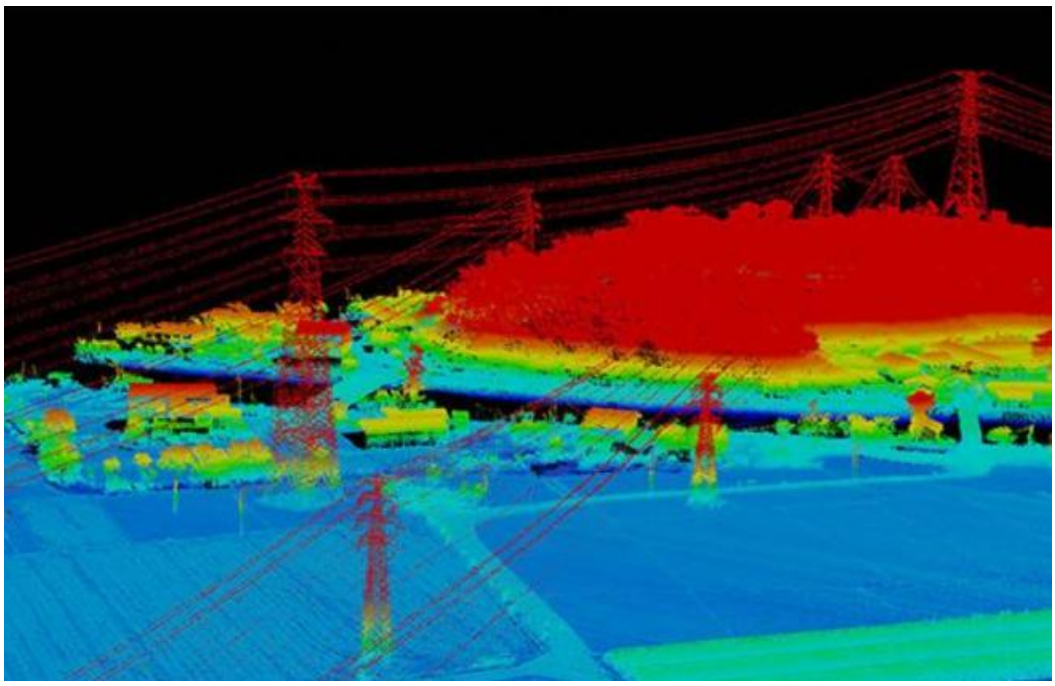

RGM combined image

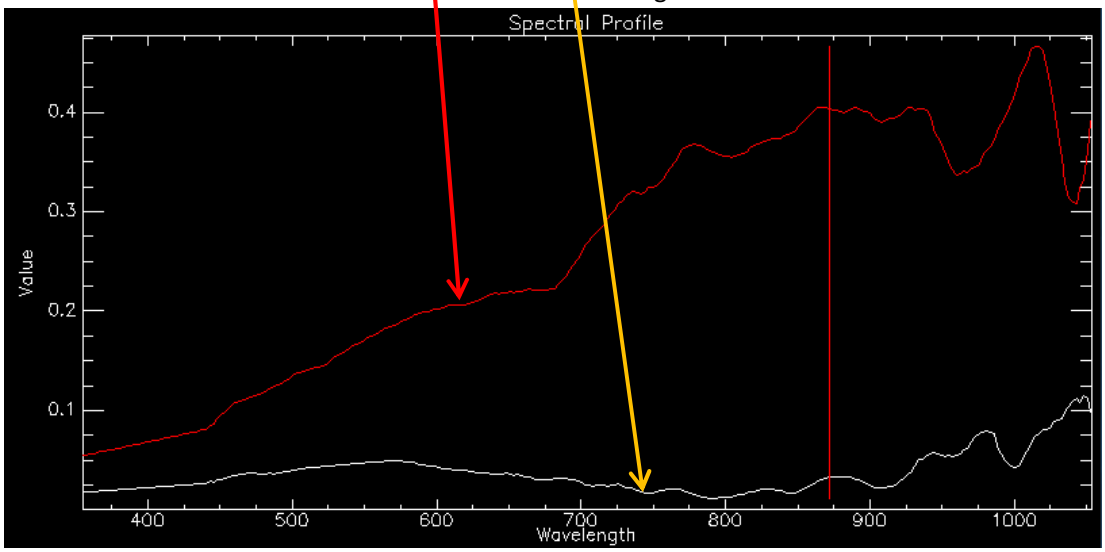

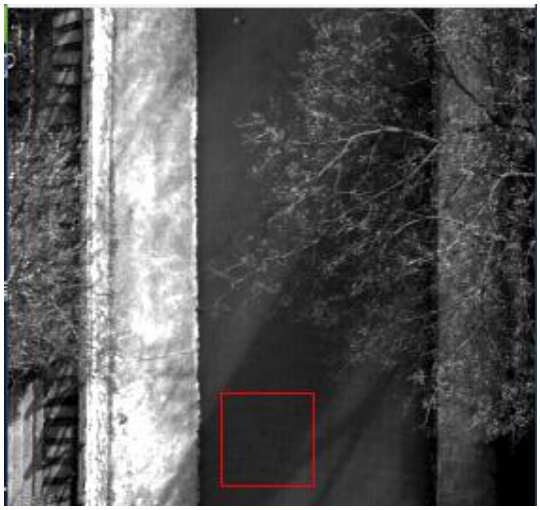

50 Band

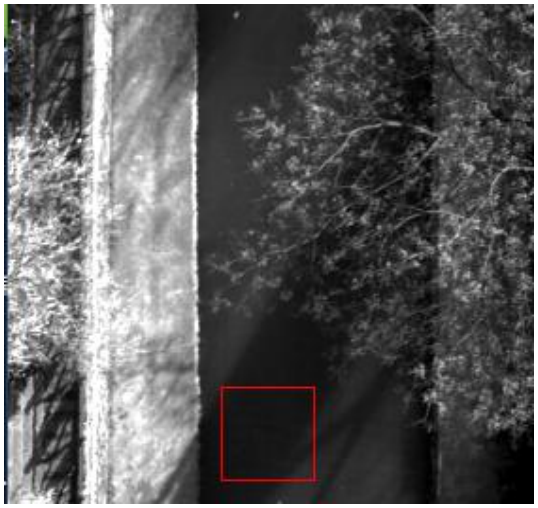

100 Band

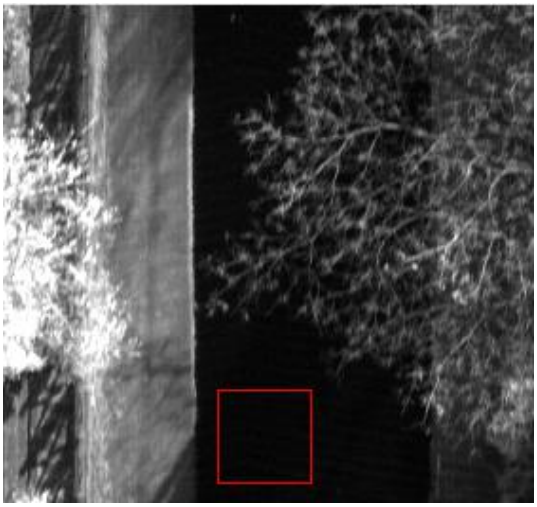

200 Band

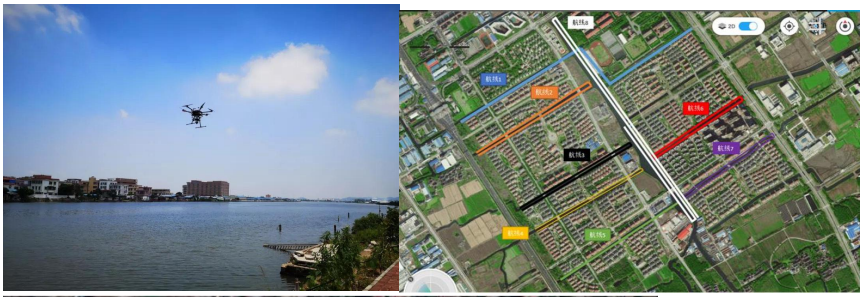

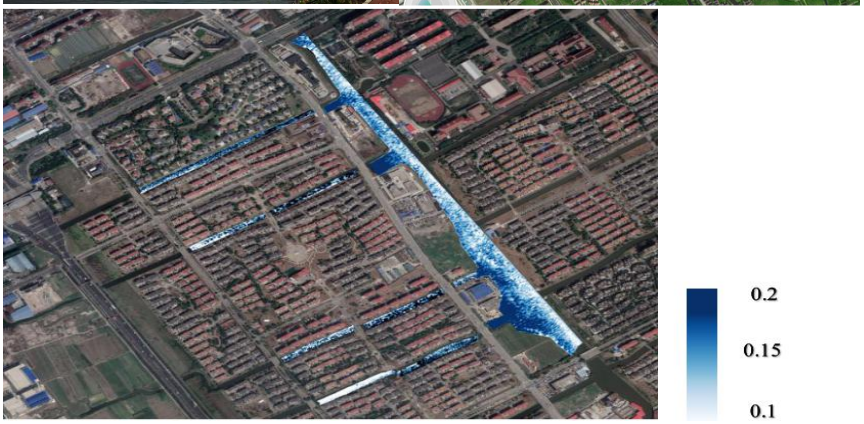

TP concentration distribution

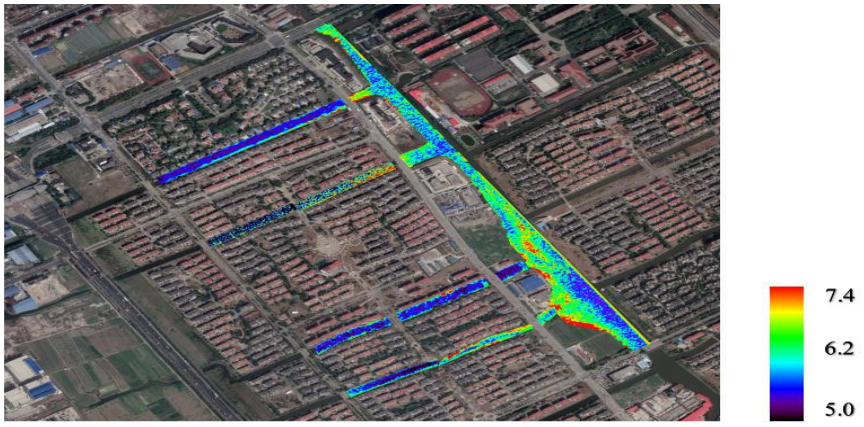

CODMn concentration distribution

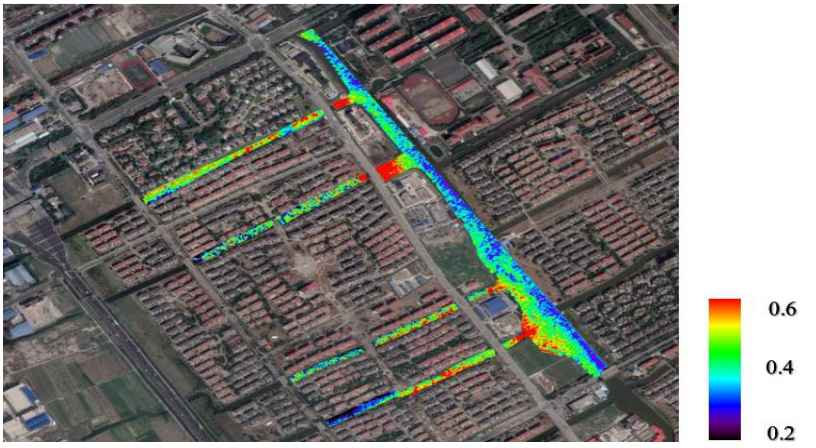

NH3-N concentration distribution

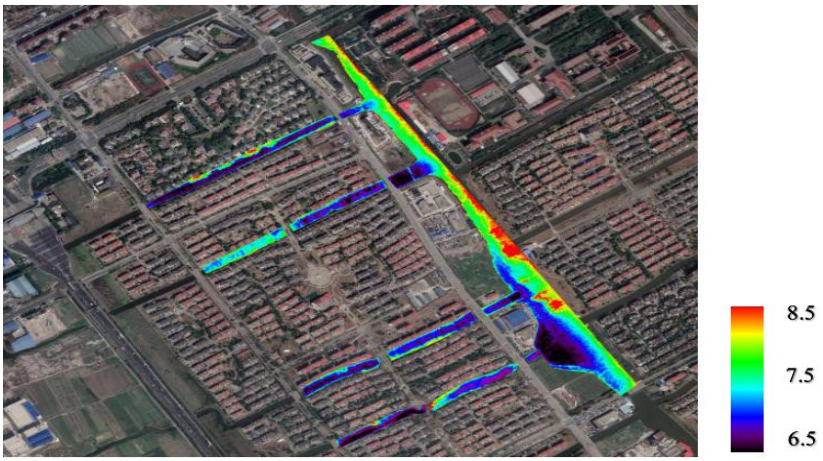

DO concentration distribution

1.2 Airborne Hyperspectral Imaging System Monitors Agriculture

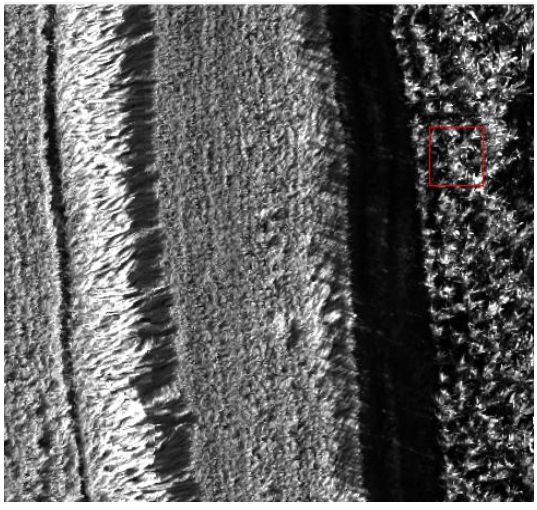

30 Band

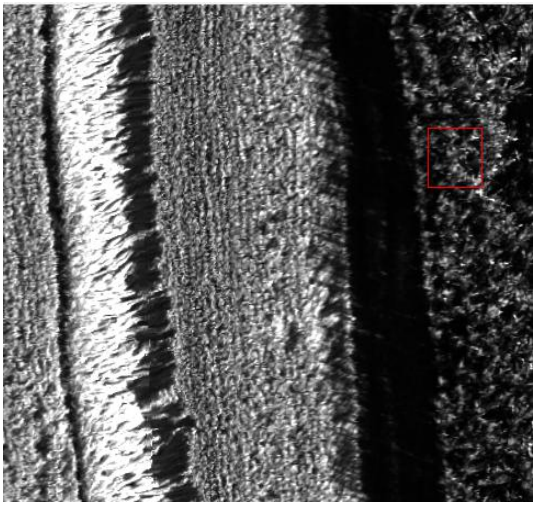

90 Band

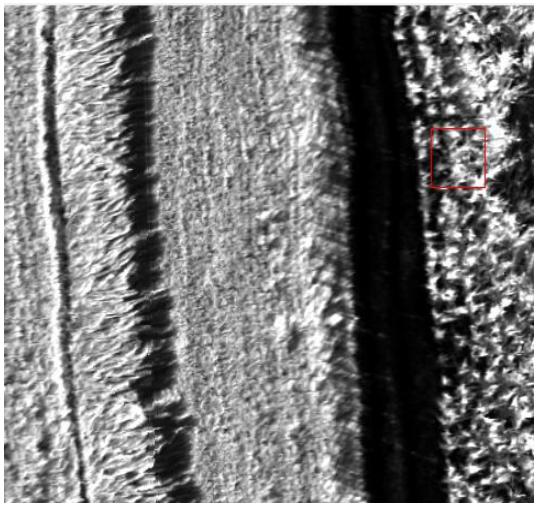

120 Band

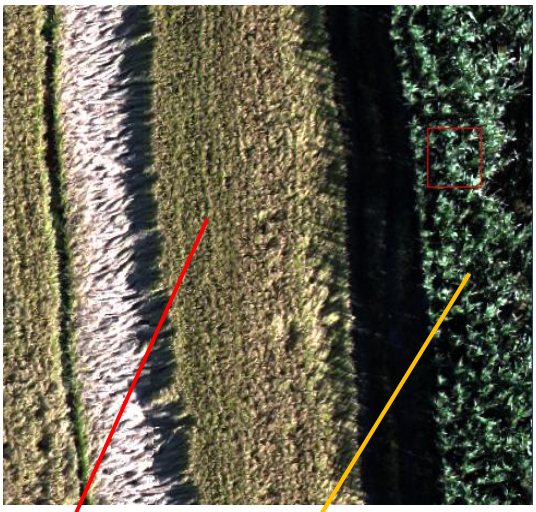

RGM combined image

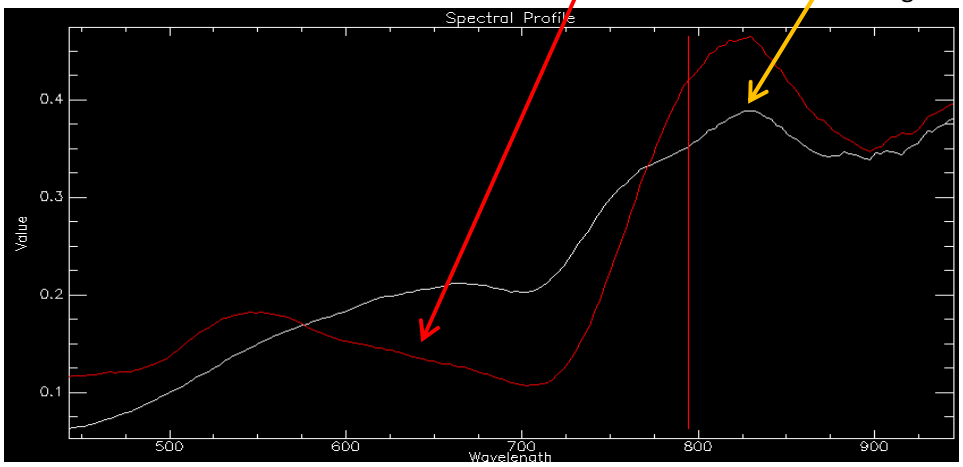

Comparison of spectral curves

1.2 Airborne Hyperspectral Imaging System Monitors Forestry

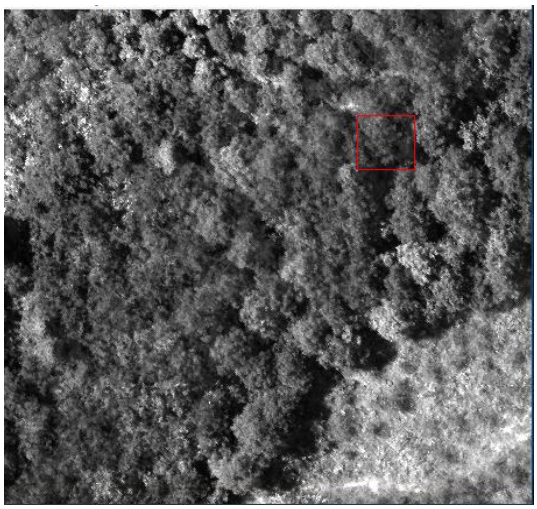

50 Band

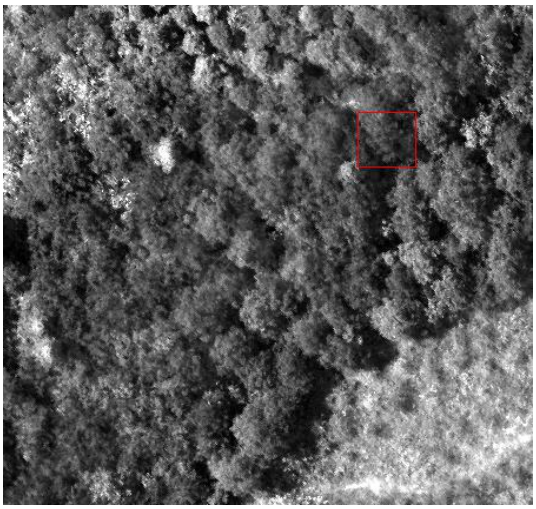

100 Band

Datasheet

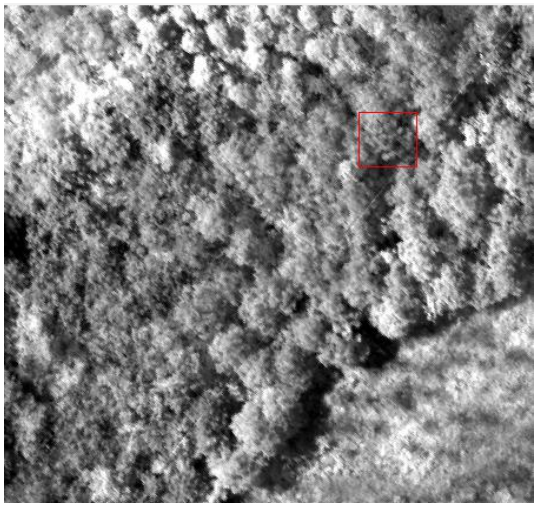

50 Band

RGM combined image

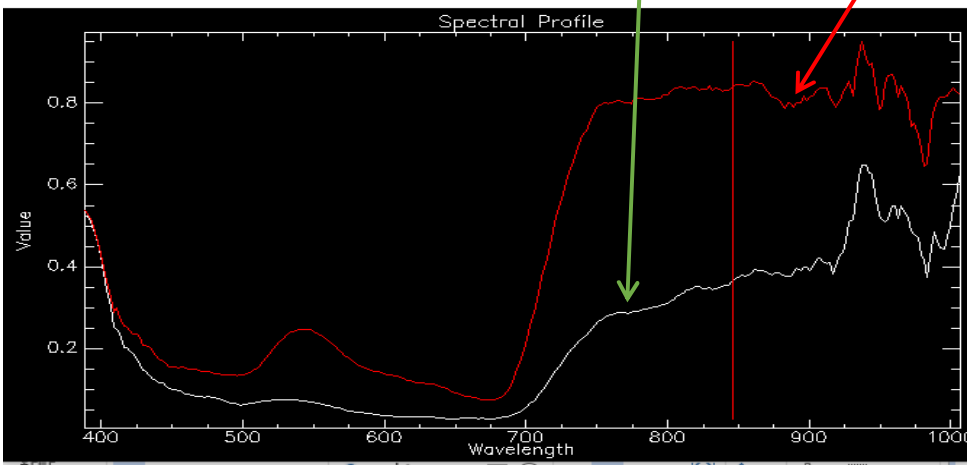

Comparison of spectral curves

orthoimage binning

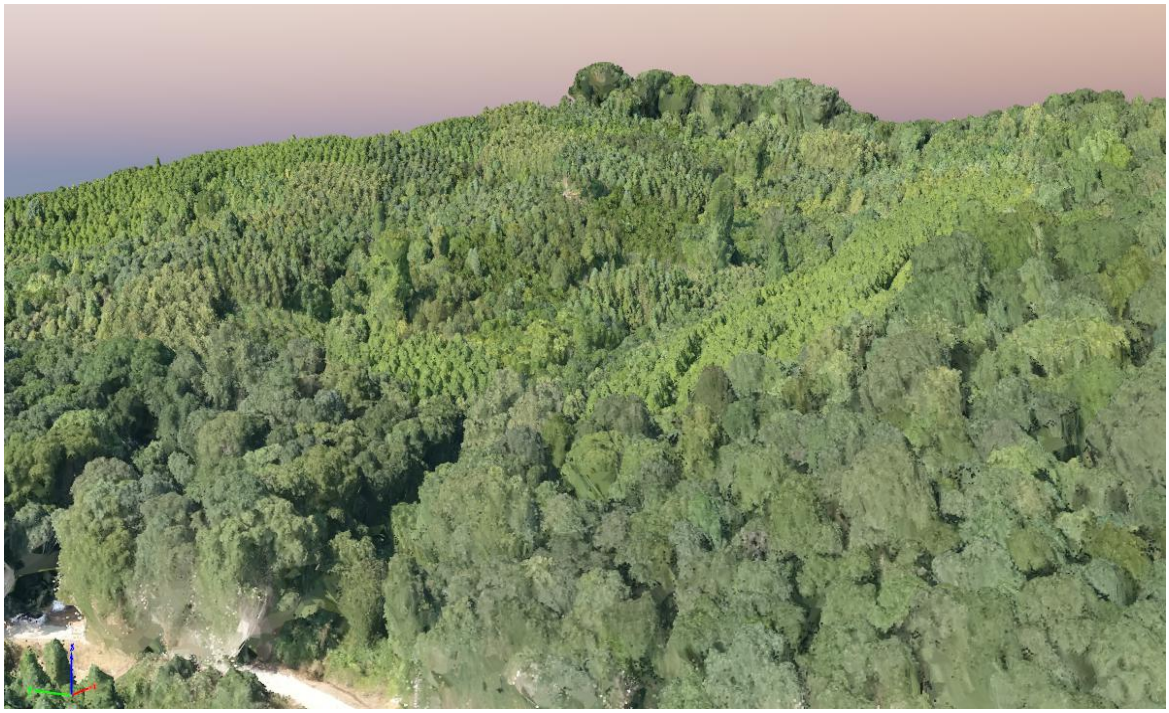

3D modeling

6. Application

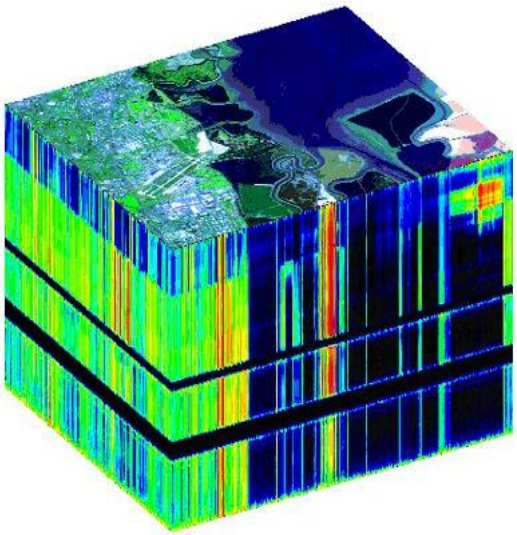

Data cube captured

Drone experiment

Outdoor experiment sceneI

Outdoor experiment sceneII

Outdoor experiment scene III

Outdoor experiment scene IV

Outdoor experiment sceneV

6.1 Industrial Sorting Application

With the development of NIR hyperspectral technology, such as Jiang tried to use near-infrared hyperspectral technology to detect impurities in cotton, especially the application of SWIR hyperspectral technology, which significantly improved the detection rate of plastic films compared with conventional methods.

Hyperspectral imaging technology is based on a very large number of narrow-band image data technology, which can obtain image information and spectral information of the sample while imaging the sample. Commonly used hyperspectral data processing methods include partial least squares (PLS), support vector machine (SVM) and artificial neural network (ANN).

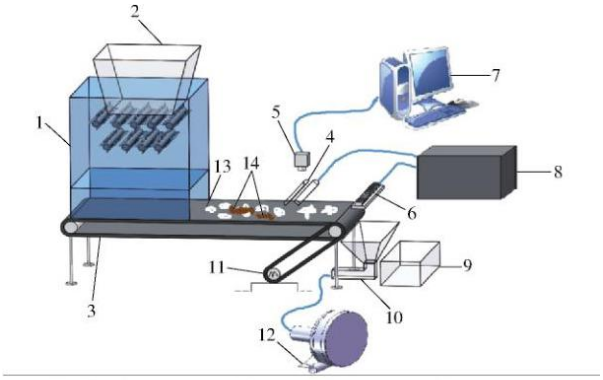

Fig. 2 Schematic of film sorting system of seed cotton

1.Cotton box 2.Cotton inlet 3.Conveyor belt 4.Dome halogen lamp
5.Hyperspectral camera 6.High speed spray valve 7.Industrial PC
8.Industrial PC 9.Seed cotton collection box 10. Waste collection box
11.Servo motor and encoder 12.Fan 13.Seed cotton 14.Film

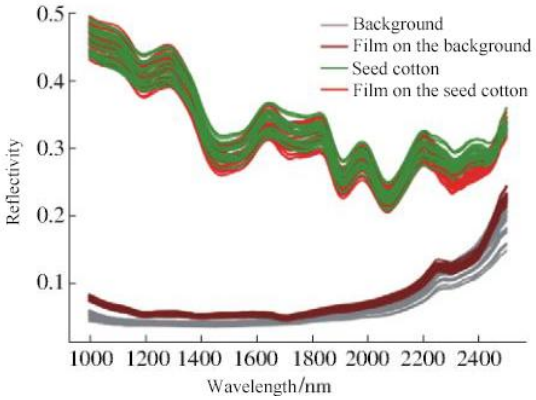

Figure 9 Seed cotton sorting application; (a) System functional composition; (b) Different substances reflectance spectrum

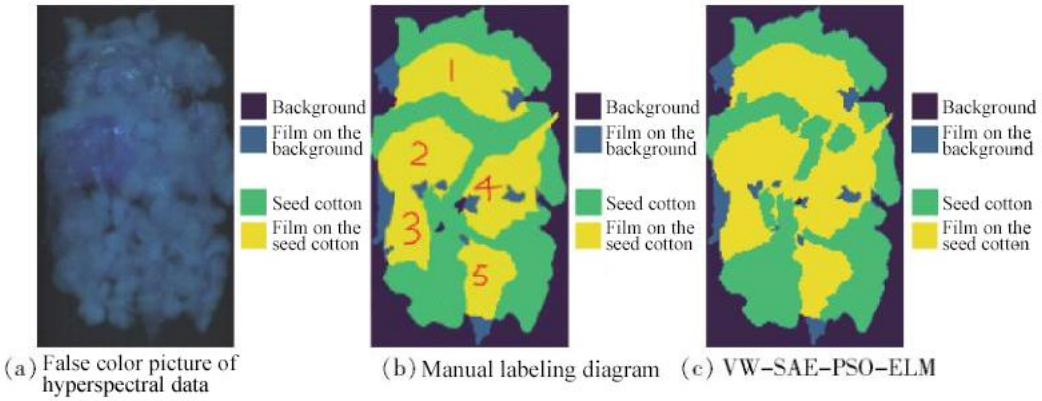

Figure 10 Seed cotton sorting application; (a) Artificial marking; (b) Recognition result

Apple's external quality is the most intuitive quality feature of Apple, which directly affects Apple's price and consumer preference. Aiming at the difficulties and key points of external inspection of apples, based on machine vision technology, hyperspectral imaging technology and multispectral imaging technology, integrated image processing technology, pattern recognition method, chemometric method and spectral analysis technology, the external physical quality of apple (shape and size) and detection methods for common defects on the surface.

The detection system and algorithm developed on the basis of the above research laid the foundation for my country's research and development of rapid online inspection and grading equipment for Apple's external quality based on machine vision technology and multi-spectral machine vision technology.

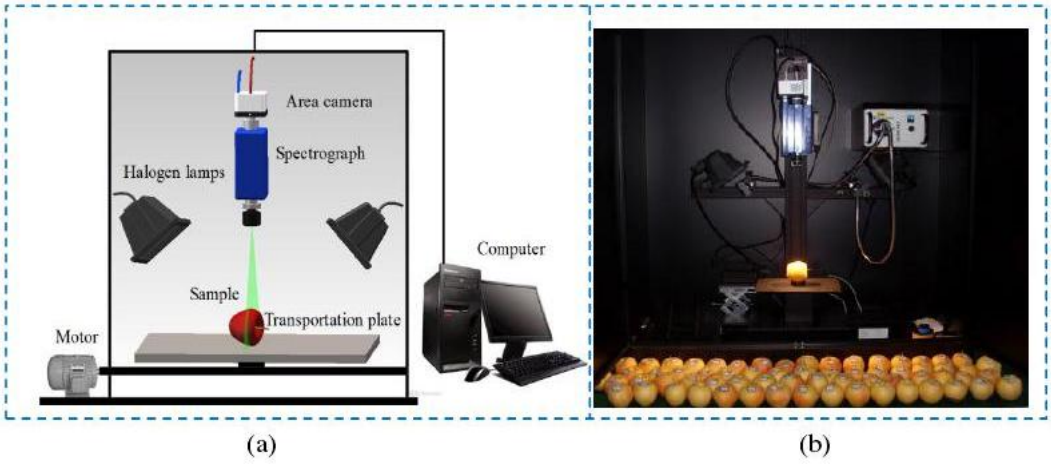

Figure 11 Schematic diagram and physical diagram developed by Dr. Zhang Baohua of Shanghai Jiaotong University; (a) Schematic diagram; (b) Physical diagram

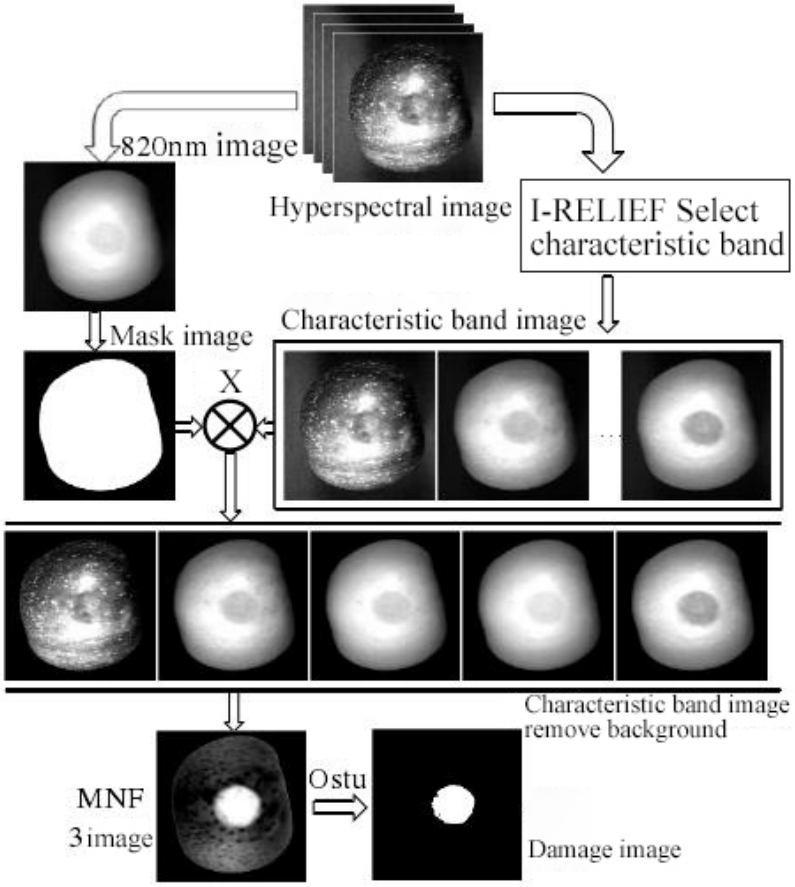

Figure 12: Flow chart of early damage detection algorithm for apple surface

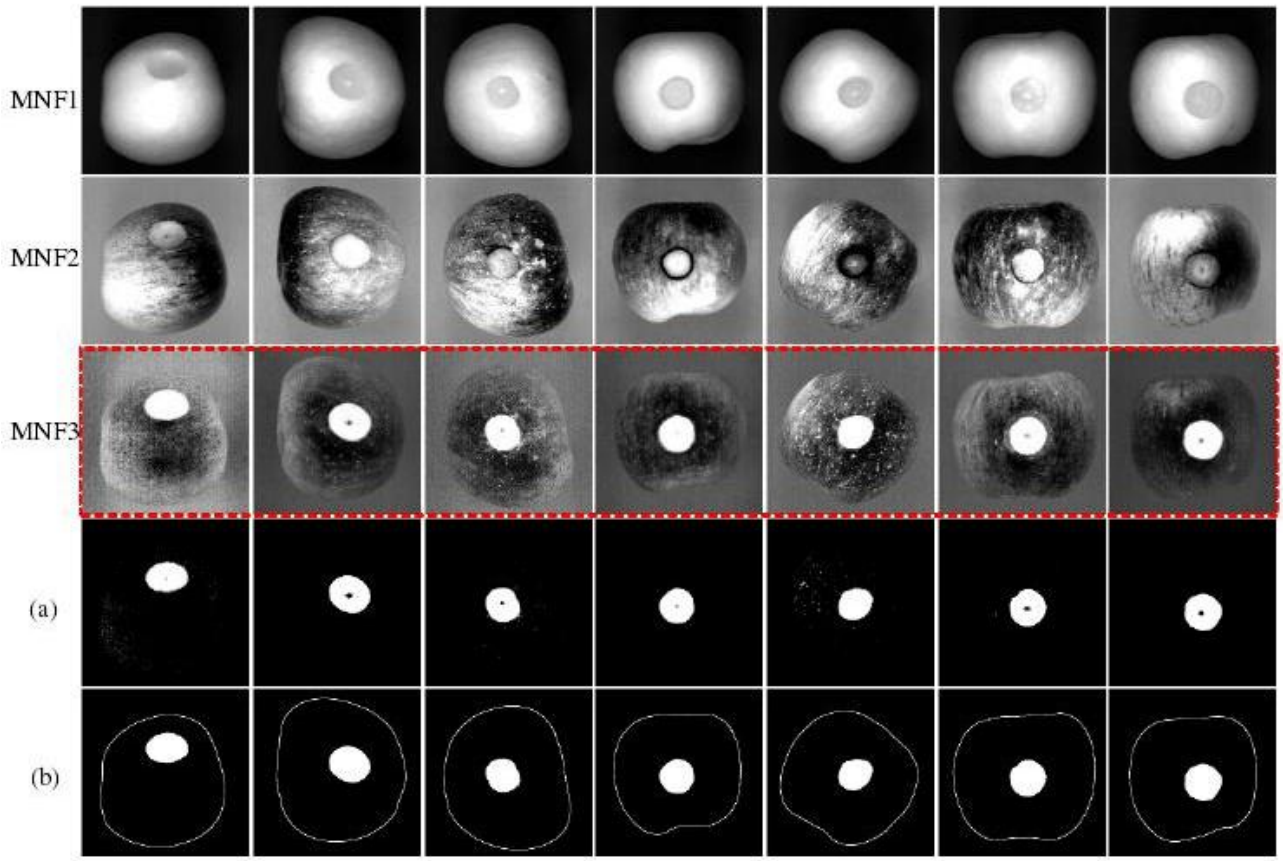

Figure 13 Recognition results of early decay of some apples and intermediate processing (a) rot segmentation results (b) final results

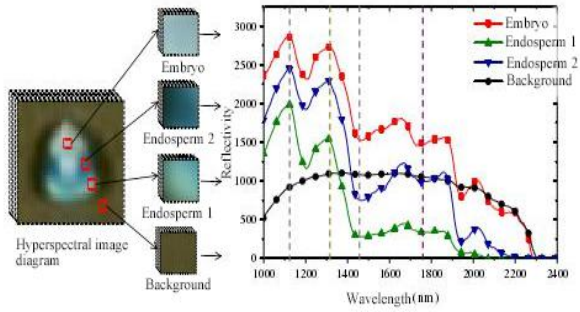

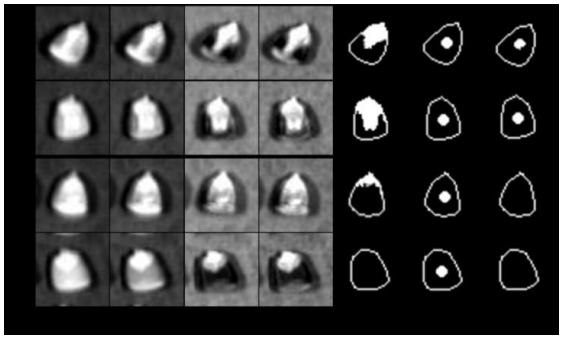

Figure 14 Corn seed sorting application (Dr. Chaopeng Wang, Northwest A&F University)

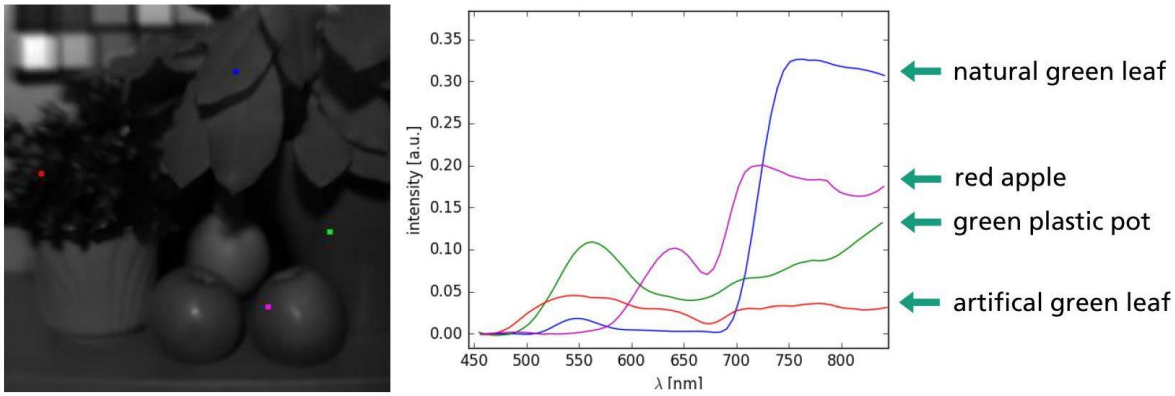

Figure 15 The spectrum of natural green plants, artificial green leaves, green plastic, and red apples

6.2 Precision Agriculture Application

Figure 16 Drone-borne hyperspectral imaging camera

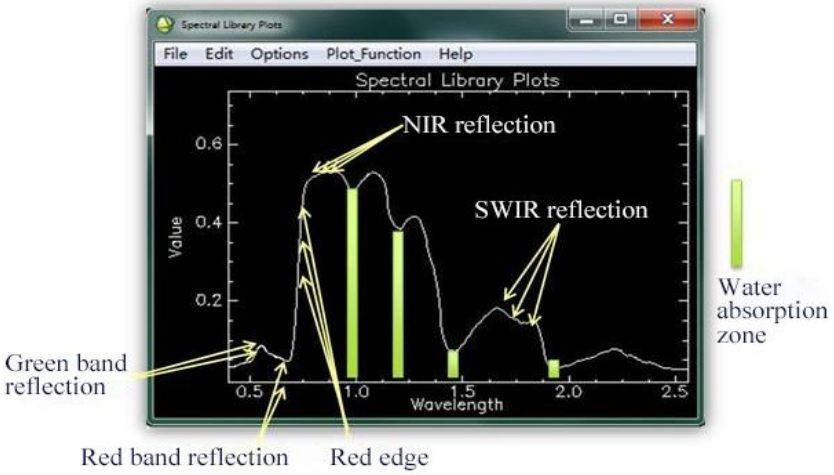

Figure 17 Green plants measured spectrum

1) **Crop growth monitoring and yield estimation:** Due to the different external factors of crops at each stage of their growth and development, there will be certain differences in their internal composition and external morphology. The most important difference is the leaf area index. Leaf area index is a comprehensive index reflecting the individual characteristics and group characteristics of crops.
2) **Crop pest control:** Remote sensing technology can monitor the effects of pests and diseases on the growth and development of crops, track the growth and development of crops, analyze and estimate disaster losses, and can monitor the distribution and activity of pests, thereby preventing the occurrence of pests.
3) **Drought monitoring of crops:** Remote sensing technology monitors crop drought conditions through crop vegetation index and canopy parameters.
4) **Monitoring of soil moisture content and distribution:** In the case of different thermal inertia conditions, the difference between remote sensing spectra is very obvious, so a mathematical model between thermal inertia and soil moisture content can be established, and remote sensing technology uses this model to analyze soil moisture content and distribution.
5) **Crop nutrient monitoring:** The accuracy of remote sensing technology to monitor the nitrogen content of crops is higher than that of other nutrient elements.

Normalized difference spectral index (NDSI), ratio spectral index (RSI) and simple spectral index (SSI) were constructed by using single band and any two bands in the range of 450 ~ 882 nm to calculate the correlation between CGI and spectral index and screen out spectral index with good correlation. Combined with partial least squares regression (PLSR), the inversion model was established.

Using CGI as the index, Airborne hyperspectral image was used to monitor the growth status of wheat in the multi-growth period in 2015. Unmanned aerial vehicle hyperspectral image inversion CGI has high precision, which can judge the difference of wheat overall growth, and can provide reference for wheat growth monitoring.

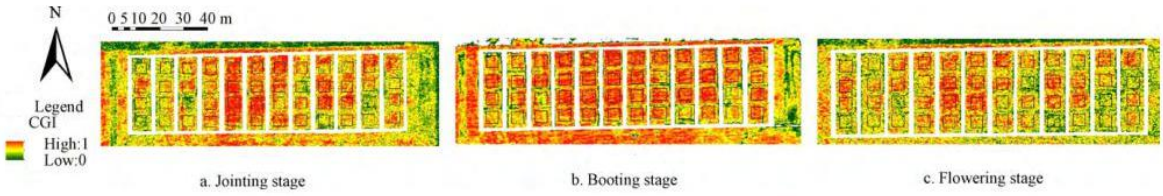

Figure 18 CGI inversion of wheat growth index

6.3 Forest Health Application

Used for pest monitoring and forest resource assessment.

Principle: The health of vegetation is related to greenness index, leaf area index, leaf moisture content and light use efficiency;

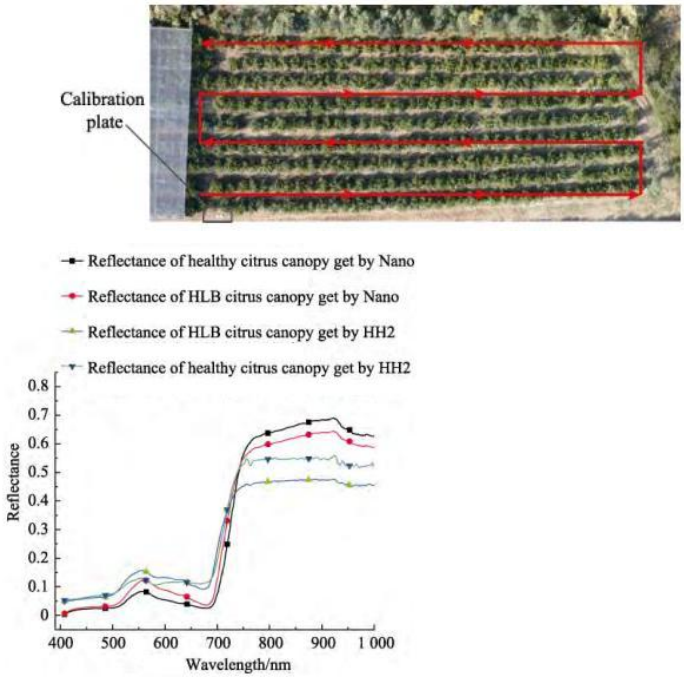

Figure 19 Monitoring and classification of citrus yellow dragon disease plants based on drone-borne hyperspectral imaging camera (designed by Lan Yubin et al., South China Agricultural University)

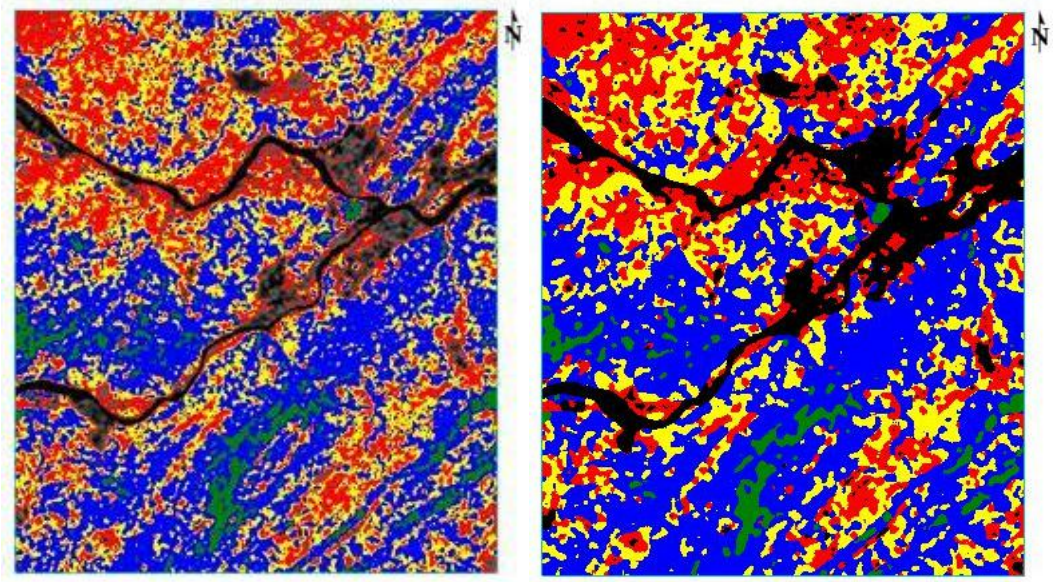

Figure 20 Distribution map of masson pine health degree studied by Wang Shuang of the University of Electronic Science and Technology of China with a hyperspectral camera

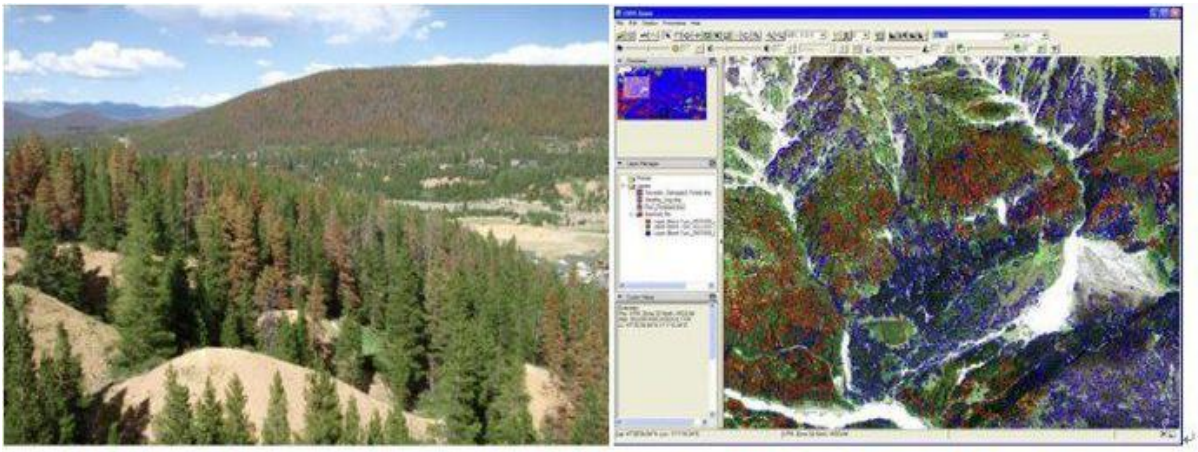

6.4 Geological Prospecting Application

Spectral remote sensing technology evolved from the multi-spectral remote sensing technology represented by Landsat and took initial shape in the mid-1980s (Goets et al., 1985, Tong Qingxi et al., 2006).

Due to its advantages of high spectral resolution and atlas integration, hyperspectral remote sensing technology has the ability of fine detection and analysis of surface rock mineral composition on a large scale. It can not only provide a macro image of the ground, but also determine the type and abundance of minerals in the geological body, and even the chemical composition of some minerals at pixel level details (Wang Runsheng et al., 2010).

In recent years, with the continuous development of hardware, data processing methods and software related to imaging spectrometer, the application of hyperspectral remote sensing technology in the field of geological survey has been accelerated.

Hyperspectral remote sensing technology has played an important role in geological mapping, the definition and division of hydrothermal alteration zones, and the delineation and

discrimination of mineralization anomalies from large metallogenic areas to medium-scale ore fields (e.g. Bierwirth et al., 2002; Company Changyun et al., 2005; Kruse et al., 2006; Cudahy et al., 2007; Wang Runsheng et al., 2010; Liu Dechang et al., 2011; Yan Baikun et al., 2014; Yang Zian et al., 2015; Graham et al., 2017).

With the theory of metallogenic system (Wyborn et al., 1994) becoming the guiding principle of prospecting practice, thematic mineral mapping on the scale of large ore concentration areas and metallogenic belts will provide key regional material composition information for predictive prospecting and exploration.

The spectral wavelength ranges used for mineral mapping include visible light (400-700nm), NIR (700-1000nm), SWIR (1000-2500nm), and thermal IR (7000-15000nm). At present, the most widely used in mining is the short-wave infrared region (1000-2500nm).

Because the frequency is close to the cofrequency and combined frequency of the chemical bond vibration in the mineral lattice, the mineral containing water or OH- (mainly layered silicate and clay) as well as some sulfate and carbonate minerals can be observed in the range of short-wave infrared wavelength.

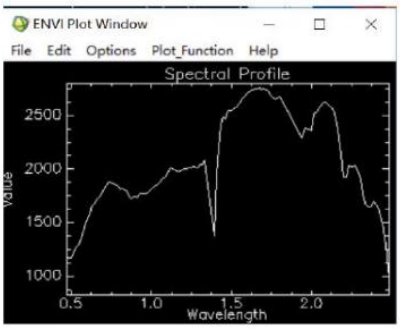

HH036 point image spectrum

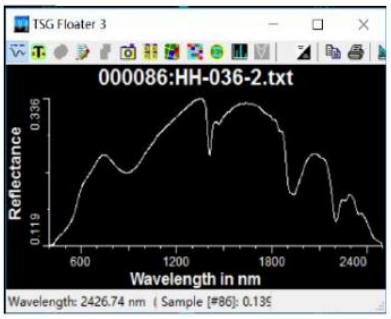

HH036 point measurede spectrum

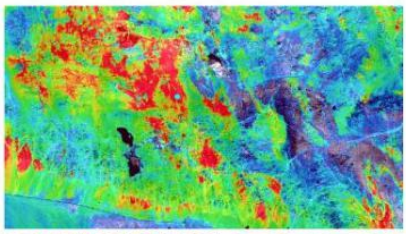

Sericite Filling Results Comparison of known deposit points between HH036 and measured

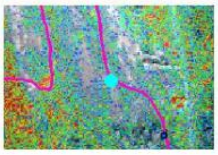

Chlorite extraction results

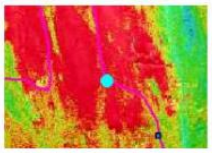

Sericite extraction results

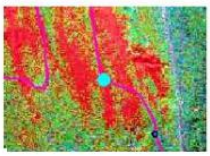

Feb3+ extraction result

Sampling point photos

Long-range photos of sampling points

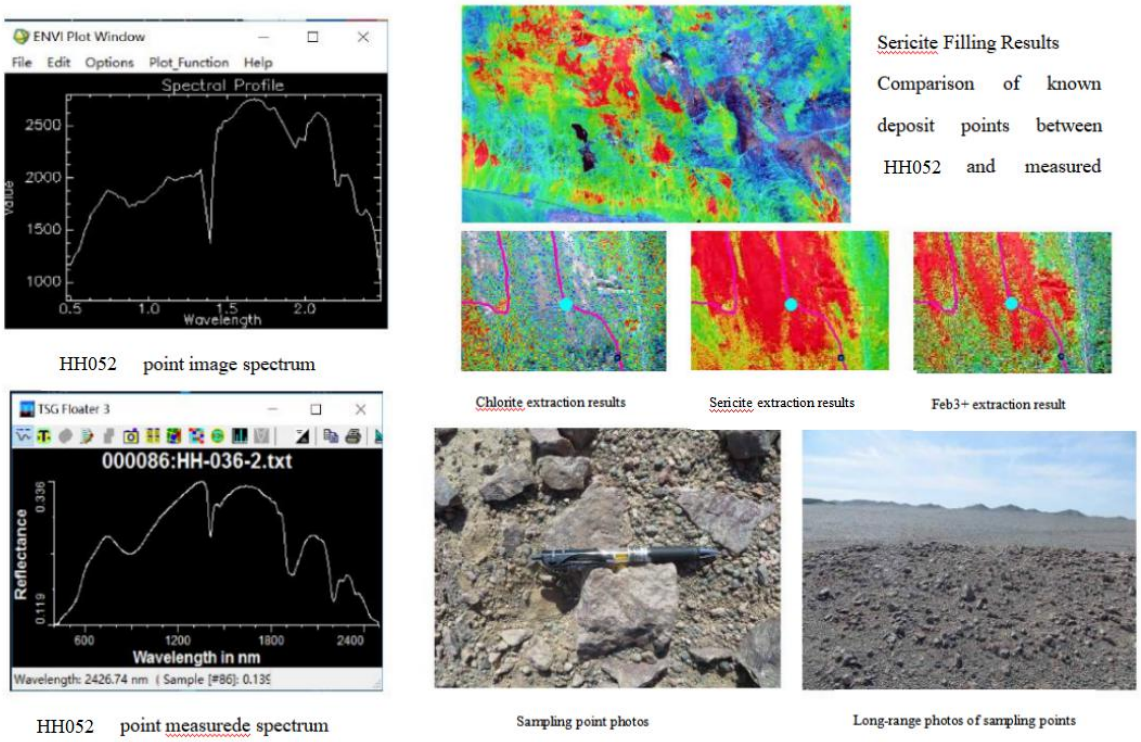

Figure 21 Application of hyperspectral imager in prospecting

Soil salinization is one of the important ecological and environmental problems in arid and semi-arid areas. Soil salinization causes soil hardening, fertility decline, acid-base imbalance, land degradation and other consequences, which seriously restricts agricultural development in China and affects the strategic situation of sustainable development in China at present.Remote sensing technology, with its characteristics of large scale, wide range, strong timeliness and economy, makes up for the deficiency of traditional methods for monitoring salinization phenomenon, and provides a new way for quantitative monitoring of soil salinization phenomenon.

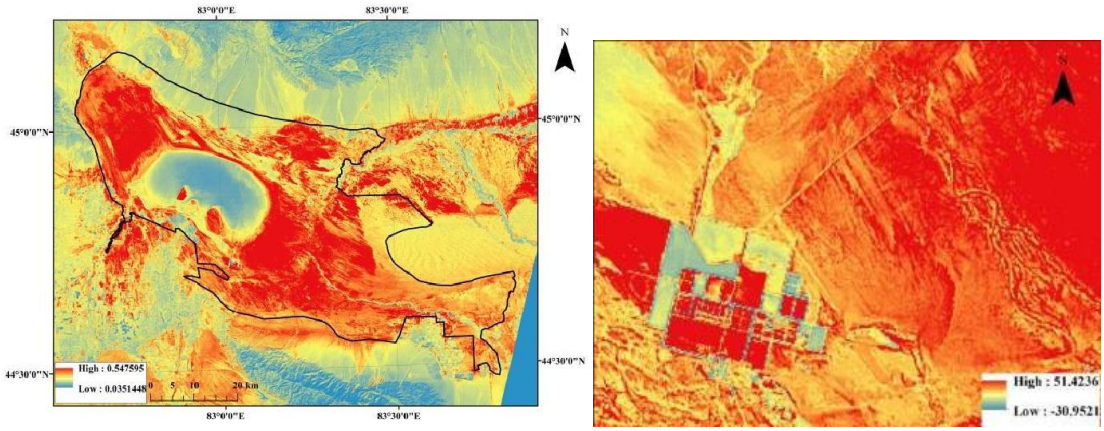

Figure 22 The surrounding area of a salt field

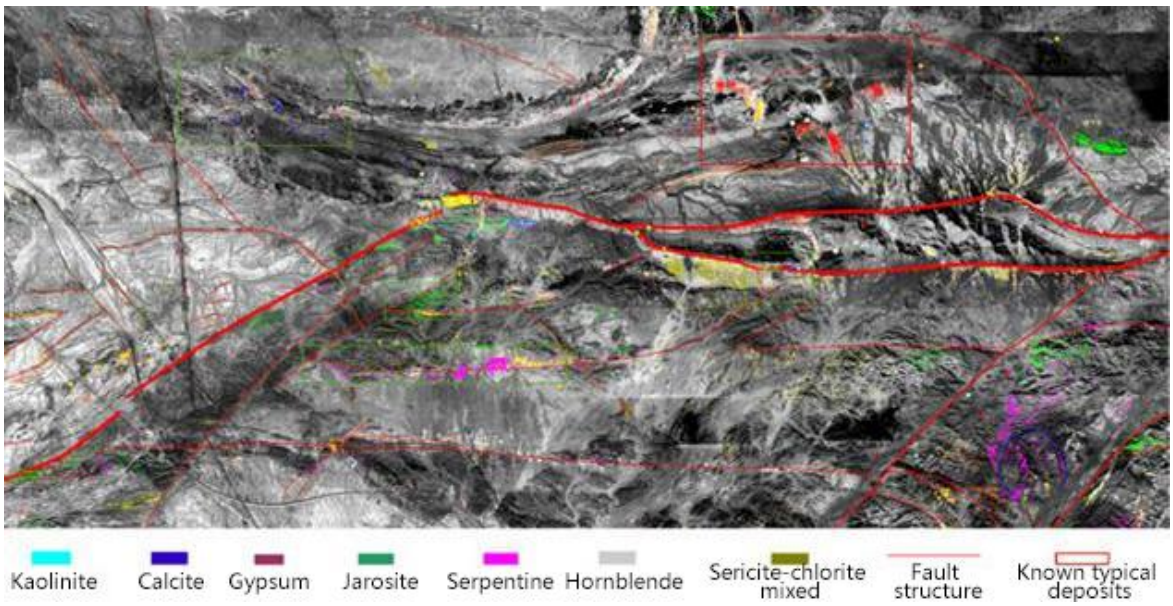

6.5 Public Safety Application

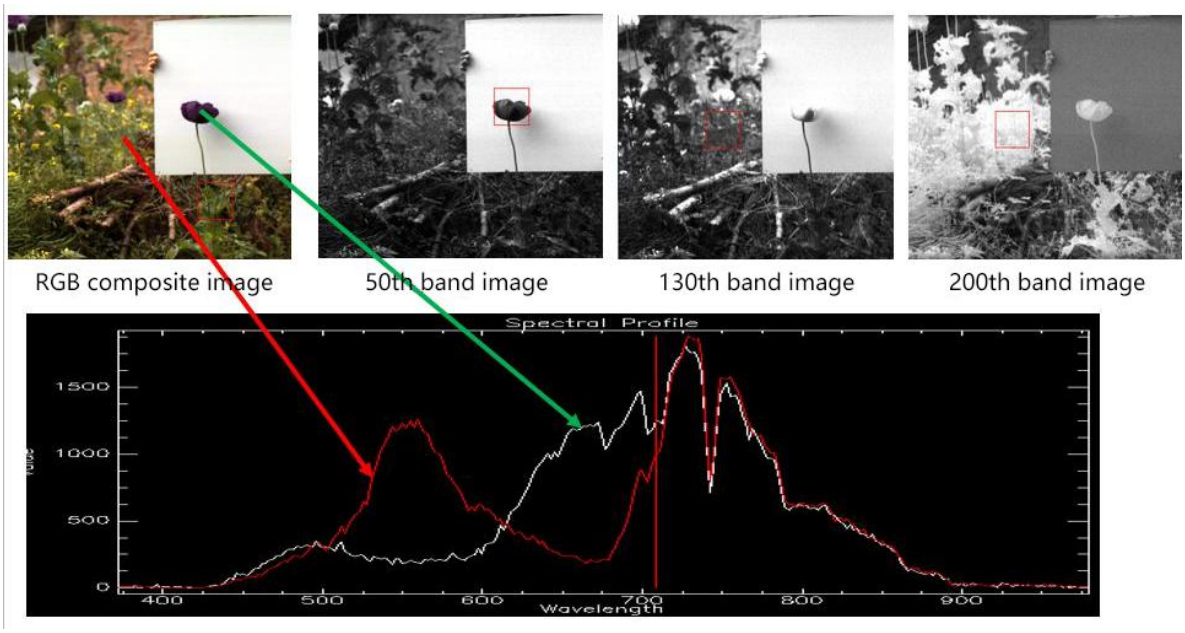

Figure 23 The searching for illegal poppy cultivation application

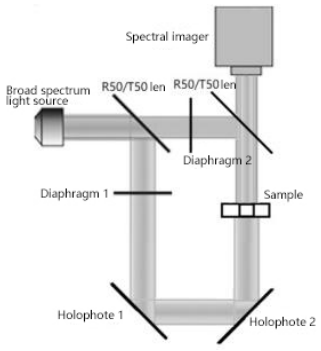

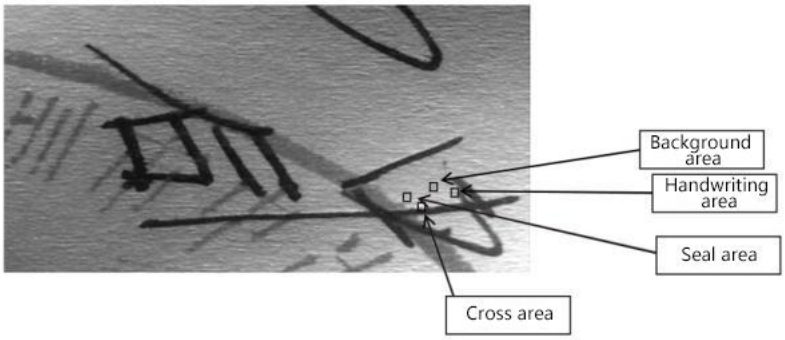

Figure 24 Document inspection application

6.6 Medical Microscopic Imaging Application

Objective: online detection and navigation positioning during tumor surgery

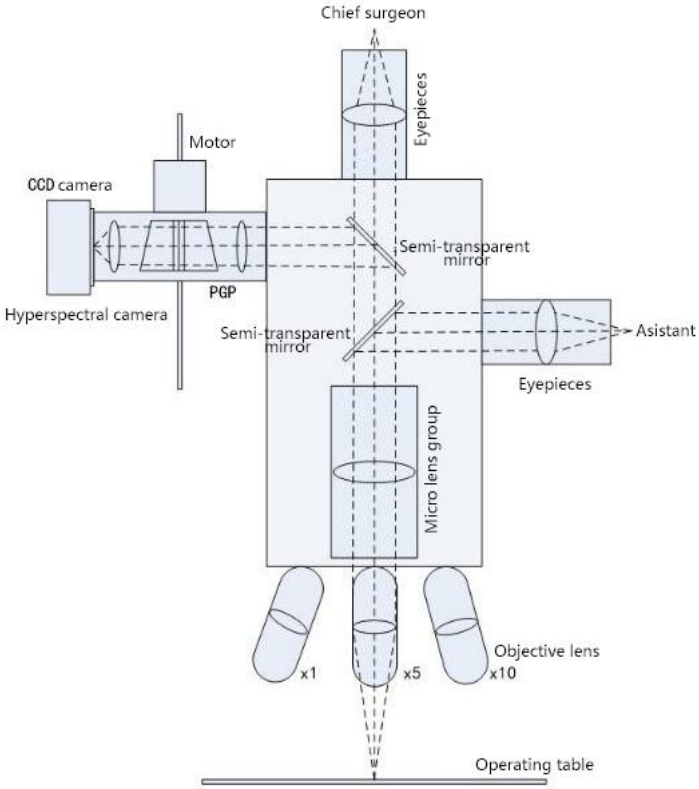

Figure 25 Medical microscope imager optical path schematic diagram

Is shown in the figure of medical microscopic imaging spectrometer principle diagram, the operating table for the target after the objective lens, microscope lens group is divided into three road, visual observation for the surgeon, all the way all the way for the assistant auxiliary visual observation, a routing imaging spectrometer detection, driven by a motor to imaging spectrometer measuring target space d scanning, imaging spectral information of the target under test, then through data analysis, image processing, through the display to the doctor.

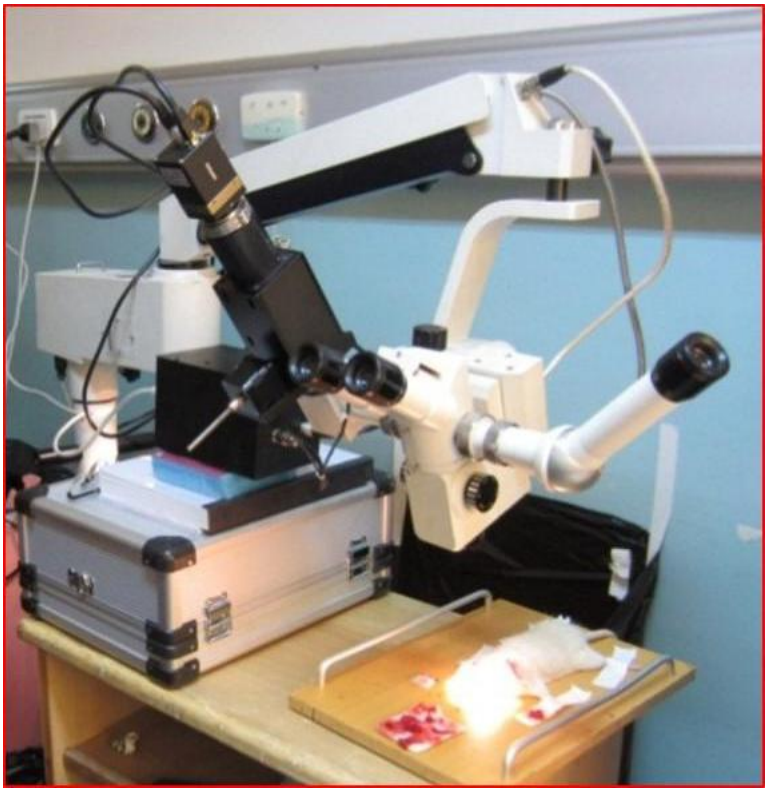

Figure 26 Medical microscope imager figure

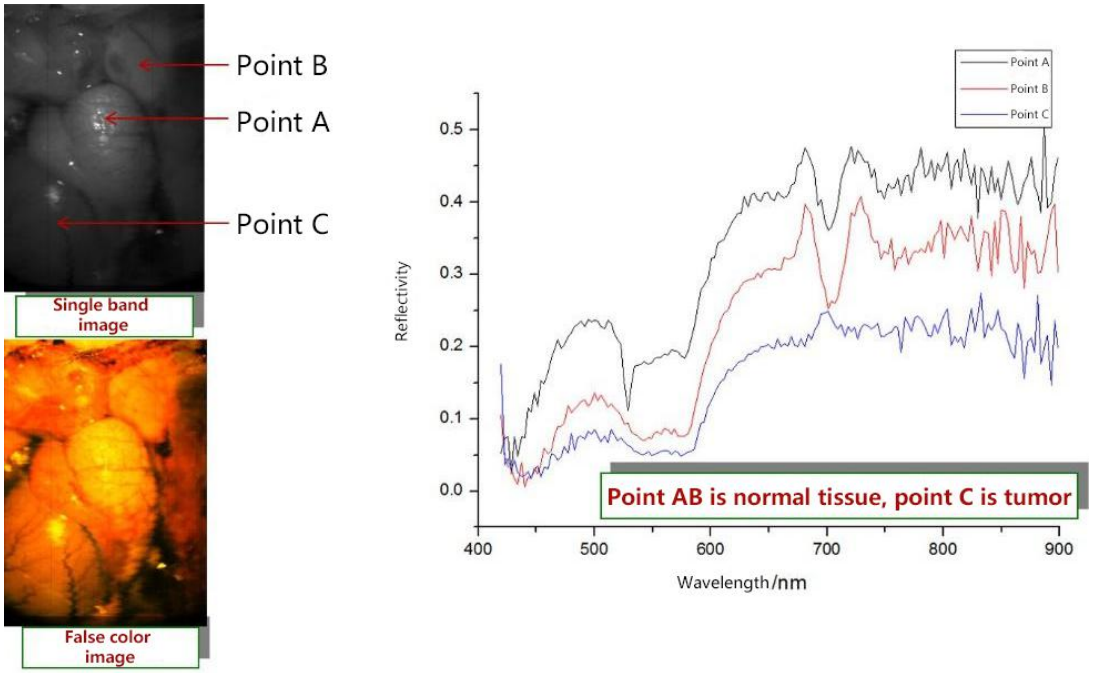

Figure 27 Data collect by medical microscopic imager

6.7 Airborne Imaging Spectroscopy Application

Figure 28 Optosky Airborne Imaging Camera

Objective: Airborne remote sensing

Application: Figure shows airborne imager consists of SpecVIEW-VIS, stable platform and POS modules. Figure 30 and Figure 31 show data was collecte. Figure 7 shows pseudo color image processed through geometric correction, flight strip spice and radiatation correction. Figure 31 shows typical geology spectral curve.

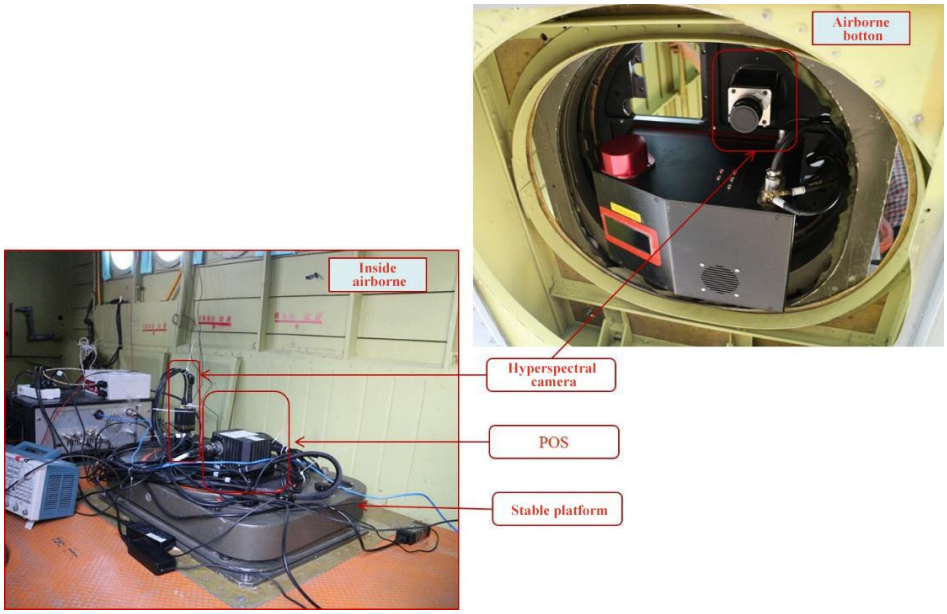

Figure 29 Airborne remote sensing application

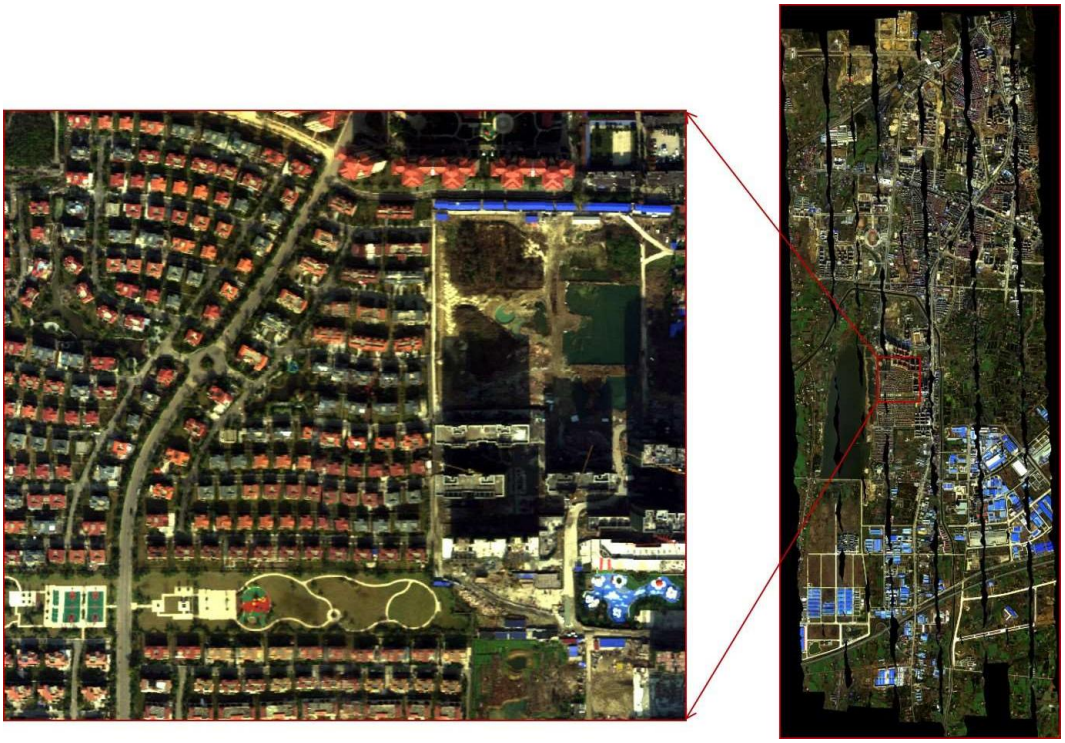

Figure 30 Airborne application data-pseudocolor image

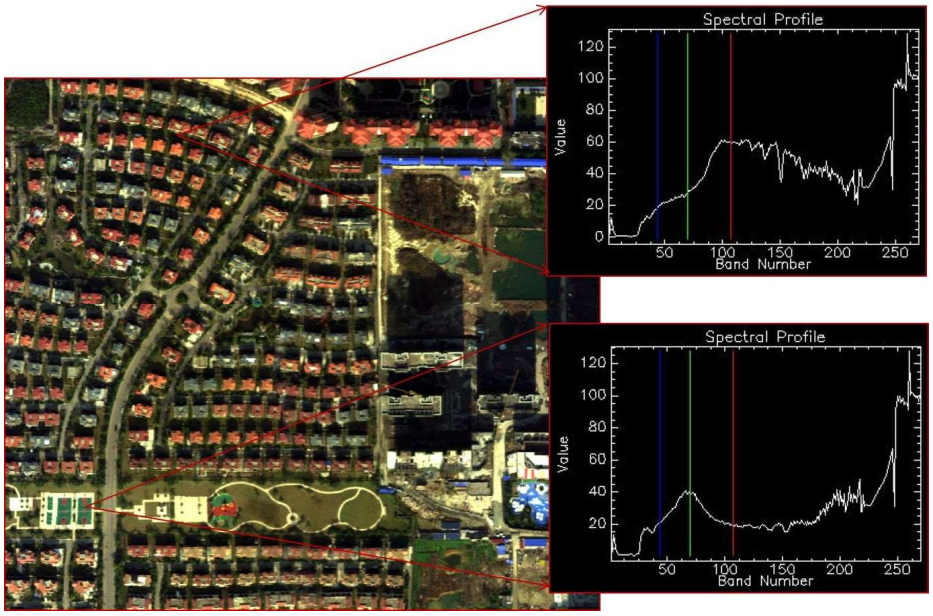

Figure 31 Airborne application data-spectral curve

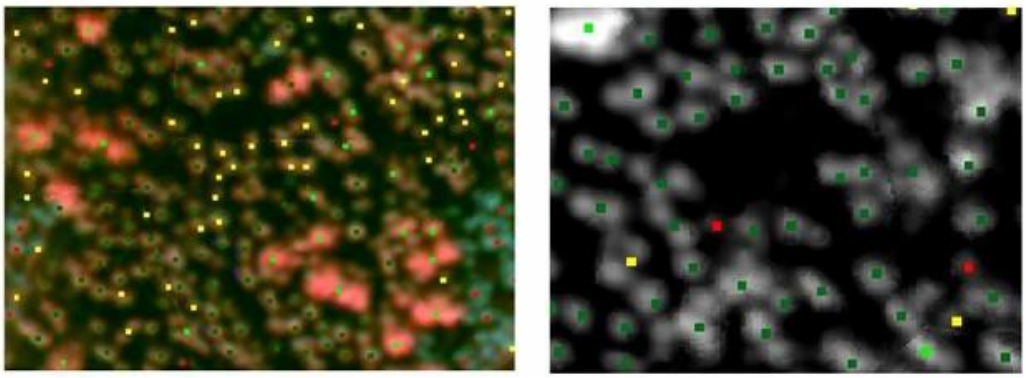

Figure 32 Forest remote sensing, Airbone hyperspectral monitor forest disease and pest

6.8 Water Quality and Environmental Protection Appication

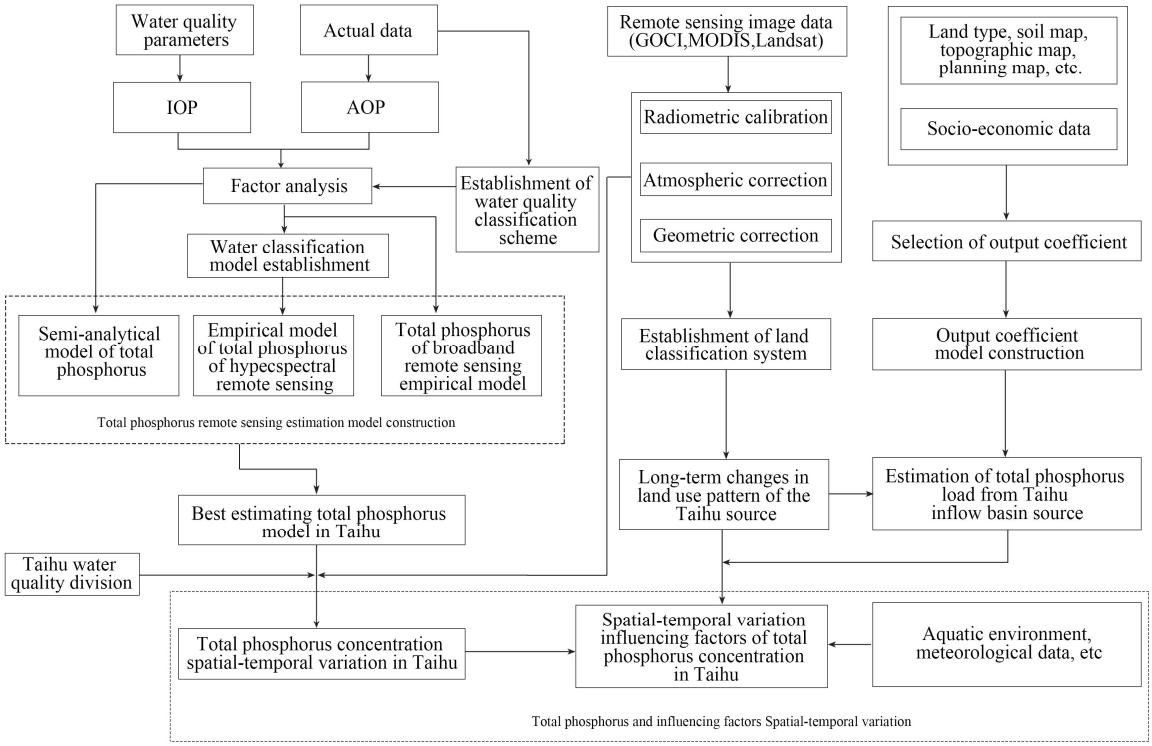

Figure 33 Inversion algorithm flow of hyperspectral data

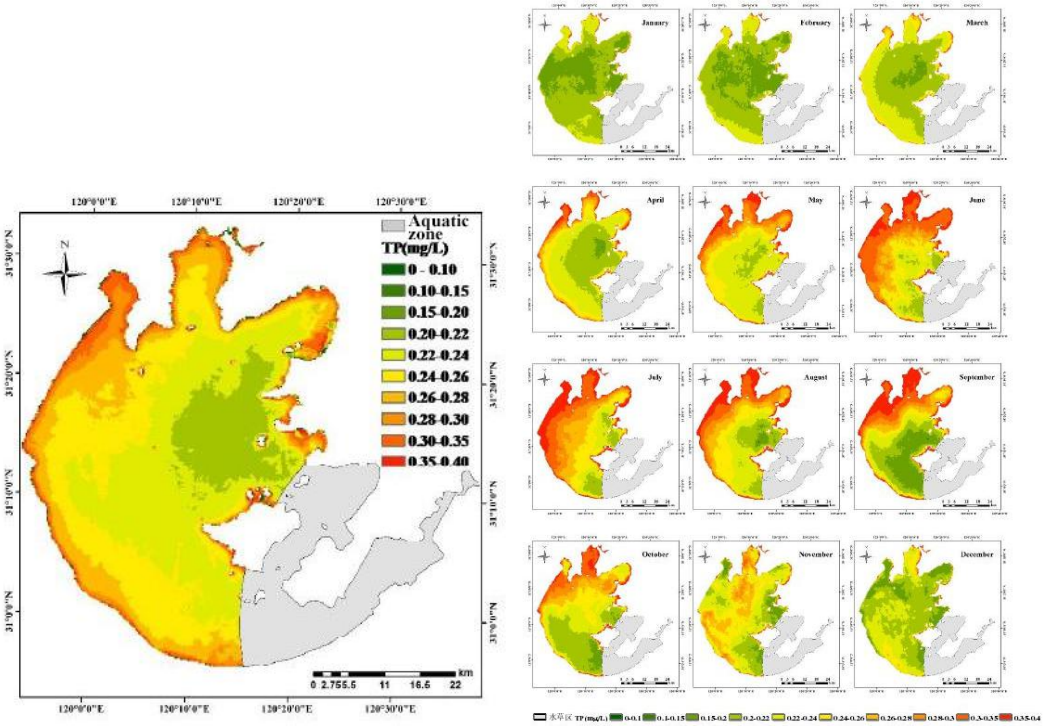

Fig. 34 (a) Spatial distribution of total phosphorus concentration in Taihu Lake. The spatial difference of total phosphorus concentration was obvious, with the highest value of 0.38mg/L and the lowest value of 0.06mg/L. (b) Monthly variation of total phosphorus concentration in different lakes.

The lake area also generally reaches its maximum phosphorus concentration between June

and September. The total phosphorus concentration in Zhushan Bay, Meiliang Bay and the west bank of Taihu Lake was higher than the mean value of the whole lake from March to October of the year, and was significantly higher than that in the rest of Taihu Lake. The total phosphorus concentration in Gonghu Bay was higher than that in the whole lake only in June, and the total phosphorus concentration in the south bank of Taihu Lake and Great Taihu Lake was relatively low throughout the year.

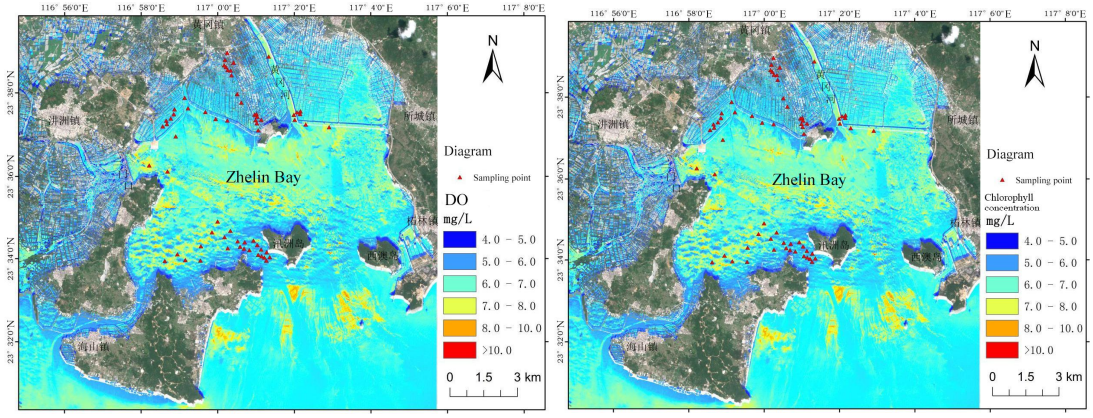

Figure 35 The distribution of dissolved oxygen and chlorophyll concentration in Zhelin Bay, eastern Guangdong, taken by hyperspectral